Bioenerg. Res. (2009) 2:246–256
DOI 10.1007/s12155-009-9054-x

Rapid Assessment of Lignin Content and Structure in Switchgrass (*Panicum virgatum* L.) Grown Under Different Environmental Conditions

David G. J. Mann · Nicole Labbé · Robert W. Sykes · Kristen Gracom · Lindsey Kline · Isabella M. Swamidoss · Jason N. Burris · Mark Davis · C. Neal Stewart Jr.

Published online: 13 October 2009

Abstract Switchgrass (*Panicum virgatum* L.) is a candidate feedstock in bioenergy, and plant breeding and molecular genetic strategies are being used to improve germplasm. In order to assess these subsequent modifications, baseline biomass compositional data are needed in a relevant variety of environments. In this study, switchgrass cv. Alamo was grown in the field, greenhouse, and growth chamber and harvested into individual leaf and stem tissue components. These components were analyzed with pyrolysis vapor analysis using molecular beam mass spectrometry, Fourier transform infrared, and standard wet chemistry methods to characterize and compare the composition among the different growth environments. The details of lignin content, S/G ratios, and degree of cross-linked lignin are discussed. Multivariate approaches such as projection to latent structures regression found a very strong correlation between the lignin content obtained by standard wet chemistry methods and the two high throughput techniques employed to rapidly assess lignin in potential switchgrass candidates. The models were tested on unknown samples and verified by wet chemistry. The similar lignin content found by the two methods shows that both approaches are capable of determining lignin content in biomass in a matter of minutes.

Keywords FTIR · Lignin · PyMBMS · S/G ratio · Cell wall · Recalcitrance

Abbreviations

ANOVA	Analysis of variance
FTIR	Fourier transform infrared spectroscopy
L1, L2, etc.	Leaf tissue 1, Leaf tissue 2, etc.
PLS	Projection to latent structures
PyMBMS	Pyrolysis vapor analysis using molecular beam mass spectrometry
RMSEC	Root mean square error of calibration
RMSEP	Root mean square error of prediction
S1, S2, etc.	Stem tissue 1, Stem tissue 2, etc.
SD	Standard deviation

Introduction

Switchgrass (*Panicum virgatum* L.) is a warm-season perennial grass native to North America, which has been targeted as an energy crop for biomass and biofuel production. It naturally possesses various traits that make it desirable as a lignocellulosic feedstock, including high yield potential, tolerance to water and nutrient limitations, low establishment costs, mitigation of soil erosion, adaptation to marginal land sites, and a high net energy gain [1–3]. While switchgrass is considered a front-running feedstock for bioenergy, the complexity of the cell wall and recalcitrance attributable to compounds such as lignin currently renders the utilization of switchgrass for ethanol production at an economic disadvan-

D. G. J. Mann · J. N. Burris · C. N. Stewart Jr.
Department of Plant Science, University of Tennessee, Knoxville, TN 37996, USA

N. Labbé (✉) · L. Kline · I. M. Swamidoss
Forest Products Center; Department of Forestry, Wildlife and Fisheries, University of Tennessee, 2506 Jacob Drive, Knoxville, TN 37996-4570, USA
e-mail: nlabbe@utk.edu

R. W. Sykes · K. Gracom · M. Davis
National Renewable Energy Laboratory, Golden, CO 80401, USA

tage [4]. Plant breeding and molecular genetic approaches can be used to decrease lignin content [5–8], and strategies are underway to produce switchgrass with modified cell walls that are more easily degraded for saccharification and fermentation [9]. Fortunately, an established tissue culture system and genetic tools exist for switchgrass [10–14], enabling trait improvements in a rapid fashion. *P. virgatum* cv. Alamo and cv. Kanlow are the only cultivars that have been described in the literature as amenable for tissue culture and transformation [10–13, 15, 16]. Alamo is a lowland variety originally isolated from Texas and has been demonstrated to have greater yields than other switchgrass varieties in the southeastern USA [17]. Hence, Alamo is the cultivar that has been selected for trait improvement within the Bioenergy Science Center, a US Department of Energy Bioenergy Center focused on addressing the recalcitrance problem that must be solved before cellulosic biofuels can be economically feasible.

To study the effects of genetic alterations of cell wall components on biomass composition, baseline data of switchgrass biomass components are needed in addition to already published papers. Differences in sugar and lignin composition have been associated with the season of harvest and plant growth stage during harvest [18–20], as well as differences between stem, leaf blade, and leaf sheath components of switchgrass [20, 21]. One study found that fiber, lignin, cellulose, hemicellulose, and ash contents have little variation among multiple varieties of switchgrass when viewed at the total dry biomass scale [17]. However, El-Nashaar et al. [22] found significantly high levels of variation in mineral composition among multiple varieties of switchgrass. Leaves tend to have lower levels of lignin and higher levels of cellulose, hemicellulose, and solubles when compared to stem components [23]. Considering different components of the stem in switchgrass cv. Kanlow, Sarath et al. [24] used high-performance liquid chromatography and gas chromatography–mass spectrometry (GCMS) and observed increased levels of cellulose and lignin in the basal internodes when compared to the apical internodes in tillers harvested at the reproductive stage. Additionally, cell solubles and hemicellulose in internodes decreased with distance from the plant shoot apex [24].

While these general trends have been observed, no single study has directly compared the compositional differences of individual components of switchgrass tillers grown in the field, greenhouse, and controlled environmental growth chambers. This information is crucial because transgenically modified switchgrass will initially be grown in environmentally controlled environments for common garden experiments for phenotypic and compositional analysis prior to being transplanted and assessed in the field. Therefore, direct comparisons between these different growth environments must be obtained.

The number of samples that need to be tested for most experiments is substantial, requiring high-throughput techniques that can rapidly screen samples of switchgrass for classification and identification of potential candidates with desirable traits. Analytical pyrolysis has been demonstrated to be a very sensitive and useful technique for the rapid analysis of plants and other biomaterials [25]. The mass spectra of the pyrolysis vapors provide a chemical fingerprint that is useful for the classification and identification of the parent material. Analytical pyrolysis is sensitive to changes in molecular, metabolite levels, and cellular structure and has been successfully used to classify microbes and other unicellular organisms [26–28]. Pyrolysis combined with GCMS (PyGCMS) has been employed to measure lignin content and determine changes in lignin structure in biomass materials [29–36]. Pyrolysis molecular beam mass spectrometry (PyMBMS) has been used to analyze the chemical composition of many different biomass materials [37–41]. More recently, PyMBMS has been employed in quantifying changes in lignin structure [42] and estimating changes in S/G ratio [42, 43]. This technique can be very informative in studies where speed is important and less detail is needed for sample assessment, e.g., traditional and transgenic plant breeding [44]. Similarly, Fourier transform infrared spectroscopy (FTIR) provides chemical fingerprints of materials in a matter of minutes. The technique is non-destructive and combined with multivariate analysis; it is a powerful tool for the rapid assessment and characterization of biological material [45]. In addition to chemical information, such as quantitatively detecting a range of functional groups, other characteristics can be retrieved from FTIR spectra, such as the index of crystallinity in cellulosic materials [46]. In this study, PyMBMS, FTIR, and wet chemistry (ASTM method) were performed to assess biomass compositional comparisons (lignin content and S/G ratio) among switchgrass cv. Alamo grown in the field, greenhouse, and growth chambers.

Methods

Plants

Switchgrass (*P. virgatum* L.) cv. Alamo plants were grown in a variety of conditions. In the field, plants were grown on the Agricultural Campus at the University of Tennessee, Knoxville, TN, USA. Switchgrass at this site was previously established by seed in 2007, and samples for this study were grown and harvested in October of 2008. Additionally, plants were grown in a greenhouse and controlled environmental chambers (Percival Scientific; Perry, IA) in Knoxville, TN in 12-L pots in Fafard 3B Mix (Conrad Fafard, Inc., Agawama, MA). In the green-

house, plants were grown at 38°C/25°C day/night temperature and 16-h day/8-h night cycle under ~300 μmol photons per square meter per second with 400-W halide lamps. In controlled environmental chambers, plants were grown at 25°C/25°C day/night temperature and 16-h day/8-h night cycle under 500 μmol photons per square meter per second with a combination of fluorescent and incandescent light. Plants in the greenhouse and controlled environmental chambers (referred to as growth chambers throughout this study) were watered with tap water and supplemented with commercial fertilizer [10–15 g 14-14-14 controlled release fertilizer every 3 months and 200 ppm of 20-20-20 soluble fertilizer biweekly (The Scotts Co., Marysville, OH)].

Harvesting of Plant Tissue

Plants at the reproductive growth stage (R1–R5 as defined by Moore et al. [47]) were harvested 4 cm above the surface of the soil and separated into (1) the flower and peduncle, (2) individual regions of the stem (included node, internode, and leaf sheath) and (3) individual leaf blades. Stem regions (S) and leaves (L) were separated by position from the top–downward (S1, S2, S3, etc. and L1, L2, L3, etc.). Once samples were separated, they were allowed to dry at 65°C for 48 h and milled in a Wiley mill through a 20-mesh screen to obtain a powder for analysis. Each sample was split with one replicate sent to the National Renewable Energy Laboratory (NREL) for MBMS analysis, and the second sample retained at the University of Tennessee for chemical analysis and FTIR analysis.

Chemical Analysis

Lignin content, the main property of interest in the study, was measured following the standard procedure developed by NREL for biomass (see website, www.nrel.gov/biomass/analytical_procedures.html). Briefly, the method employs a two-step acid hydrolysis to fractionate the biomass (carbohydrates and lignin) into forms that can be quantified. Lignin was fractionated into an acid-soluble and acid-insoluble fraction. The soluble lignin fraction was measured by UV-Vis spectroscopy, while the insoluble fraction, which might contain ash and protein, was quantified by gravimetric analysis. Each switchgrass sample was analyzed in triplicate.

Pyrolysis Vapor Analysis Using Molecular Beam Mass Spectrometry

A custom-built molecular beam mass spectrometer using an Extrel^{TM} Model TQMS C50 mass spectrometer was used for pyrolysis vapor analysis [48, 49]. Minor modifications were made to incorporate a commercially available autosampler inlet pyrolysis system. The autosampler furnace was electronically maintained at 500°C, and the interface was set to 350°C. The 3.2-mm transfer line was wrapped in heat tape and heated to approximately 350°C measured with thermocouples. Helium gas (2 L/min) was used to carry the pyrolysis vapors from the pyrolyzer to the mass spectrometer. The residence time of the pyrolysis vapors in the reactor pyrolysis zone has been estimated to be ~75 ms and is short enough that secondary cracking reactions are minimal.

Samples of approximately 4 mg were introduced into the quartz pyrolysis reactor via 80 μL deactivated stainless steel Eco-Cups (Frontier Lab, Ltd.). Samples were randomized throughout the experimental run to eliminate bias as a result of possible spectrometer drift. Disks of glass fiber filter paper (type A/D) cover the top of the sample to prevent sample from coming out of the cup during injection. Mass spectral data from m/z 30–450 were acquired on a Merlin Automation data system version 2.0 using 22.5 eV electron impact ionization.

S/G Ratio Estimation

S/G ratios were determined by summing the intensity of syringyl peaks 154, 167, 168, 182, 194, 208, and 210 and dividing by the sum of the intensity of guaiacyl peaks 124, 137, 138, 150, 164, and 178 [43]. Several lignin peaks were omitted in the syringyl or guaiacyl summations as a result of individual peaks having associations with both S and G precursors.

Fourier Transform Infrared Spectroscopy

Switchgrass powder was placed on a ZnSe crystal of an attenuated total reflectance accessory of a Perkin-Elmer Spectrum One FTIR spectrometer. Spectra were collected over 4,000–650 cm^{-1}, with the resolution of 1 cm^{-1} and eight scans per sample. Sample contact area was a circle of about 1.5 mm in diameter. Five spectra were collected for each switchgrass sample. In total, 15 spectra were collected for each switchgrass tissue.

Cross-Linked Lignin Ratio

Absorbance ratios between peaks around 1,500 and 1,600 cm^{-1} were calculated to estimate the relative level of cross-linked lignin present in the biomass. The more condensed and cross-linked the lignin is, the higher this ratio will be.

Data Analysis

Student t test was used for analyzing standard wet chemistry results. ANOVA was conducted on lignin measurements from wet chemistry, S/G ratios from

MBMS, and lignin cross-linking absorbance ratios from FTIR using SAS (Mixed procedure, 2008, SAS Institute. Inc., Cary, NC), and least squares means were compared. Letter groupings were obtained using Fisher's least significant difference method where $P \leq 0.05$. Using this method, no common letters between samples indicate that there is a significant difference between the samples being compared.

The FTIR and MBMS spectral data were imported into The Unscrambler software (ver. 9.2; CAMO A/S, USA) for model development. The FTIR spectra were mean normalized and subjected to a full multiplicative scatter correction to compensate for multiplication and/or additive scatter effects in the data. The MBMS spectral data were mean normalized prior to the analysis. Multivariate analysis was used to extract useful information from the spectral data set. Projection to latent structures (PLS) was performed to develop a model to predict lignin content. PLS provides a model for the relationship between a set of predicator variables *X* (spectral data) and a set of response variables *Y* (lignin content). If the spectral data contain information about the property of interest, a reliable calibration model can be constructed. The models were validated using a full cross-validation approach. In this technique, a sample is excluded from the data set and the model is calculated on the remaining data points. The value for the excluded sample is then predicted. Reiterations permuting each sample are performed until every object has been excluded once. This approach is used to assure that the developed models are not over-fitted (a tendency to describe too much of the variation in the data, where not only consistent structure is taken into account but also some noise or uninformative variation). The number of principal components (factors) used for the models was selected by observing the response of the residual *Y* variance to added factors. The models were completed when additional factors did not substantially decrease the residual *Y* variance. PLS models generate also regression coefficients, or information on the chemical features that drive the calibration. The regression coefficients are useful to relate chemical features in the spectra to the properties of interest.

Results

To study the effects of growth environments on switchgrass biomass composition, and more specifically on lignin content, plants were grown in the field, greenhouse, and environmentally controlled growth chambers. Plants were then divided into different components (Fig. 1), and individual leaves (L1 to L7) and stem regions (S1 to S7) were analyzed. Different growth patterns were observed by the percentage of biomass component (leaves versus stem) obtained for each growth environment (Fig. 2). Plants grown in the field had the highest percentage of stem and lowest percentage of leaf biomass (75% and 25%, respectively), while plants grown in the growth chambers had the lowest percentage of stem and highest percentage of leaf biomass (56% and 44%, respectively). The biomass of plants grown in the greenhouse was in between these values (65% for stems and 35% for leaves). Although the percentage of biomass components fluctuated from one growth environment to another, there were no significant differences observed between the average number of nodes per tiller across all three environments (data not shown).

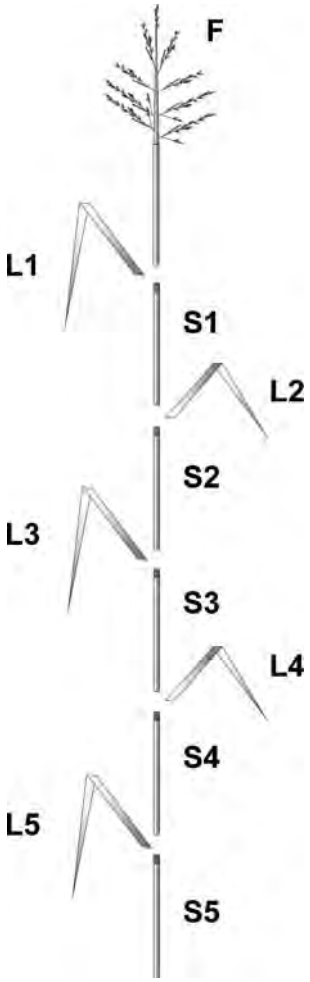

Fig. 1 Representation of individual tiller components of switchgrass as indicated in the analysis. Tiller components are indicated by letter: *F* flower, *L* leaf blade, *S* stem tissue

Individual leaf and stem tissues for switchgrass grown in field and greenhouse environments were analyzed using standard wet chemical method (wet chemistry; Table 1). For field samples, there were significant differences when comparing the total stem and total leaf tissues for xylose, arabinose, mannose, ash, and lignin content ($P \leq 0.05$). For the greenhouse samples, there were significant differences

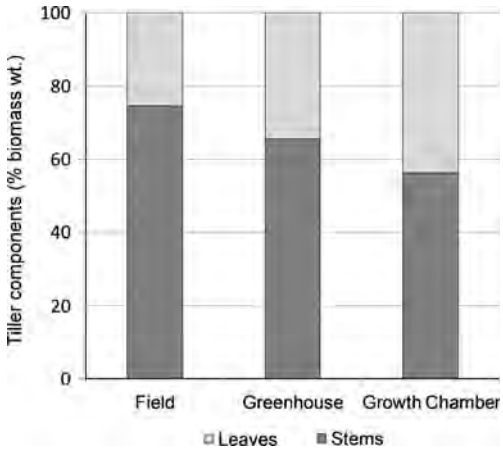

Fig. 2 Allocation of biomass to leaves and stems of tillers harvested from the field, greenhouse, and growth chamber, as measured by the total percentage of biomass weight

between the total stem and the total leaf tissues for glucose, xylose, arabinose, ash, and lignin contents ($P \leq 0.05$). Additionally, significant differences were observed when comparing individual tiller components for the field versus the greenhouse (Table 1). While some differences were detected for sugar content (e.g., the glucose, xylose, and galactose content in leaf 1), the most striking differences were observed in the ash contents between switchgrass from the field and switchgrass from the greenhouse, with the field samples having significantly more ash content in the young leaves (L1, L2, and L3) and significantly less ash content in the lower leaves (L4 and L5) and stem tissues (S1, S2, S3, and S4) when compared to the greenhouse.

Because the characterization of biomass is time consuming, spectroscopic approaches were employed to rapidly analyze the numerous samples. Figure 3a and b show FTIR and MBMS spectra collected on leaf (L1) and stem (S1) of switchgrass plants grown under the three different environments (field, greenhouse, and growth chamber). While some small differences can be observed, the various tissues possess similar spectral profile. In the mid-infrared spectra, bands are observed at 3,340, 2,920, 2,850, 1,735, 1,635, 1,603, 1,515, 1,463, 1,427, 1,371, 1,320, 1,245, 1,160, 1,035 and 899 cm^{-1}. Some of these bands are functional bands found in the main constituents of switchgrass

Table 1 Wet chemistry analysis for characteristics of switchgrass components

	Glucose	Xylose	Galactose	Arabinose	Mannose	Ash	Lignin	Extractives
Field								
Leaf 1	32.4±0.4*	20.7±0.3**	2.94±0.02*	2.65±0.17	0.99±0.68	6.13±0.08*	13.7±0.4*	17.4±0.2
Leaf 2	30.0±0.9	17.9±0.6	2.54±0.33	2.10±0.28	0.61±0.13	5.07±0.08**	14.2±0.9	21.0±0.7
Leaf 3	33.1±0.1	20.3±0.2	3.05±0.24	2.77±0.08	0.62±0.14	5.32±0.06**	14.0±0.4	16.6±0.1
Leaf 4	30.5±0.7	19.6±0.5	3.10±0.19	2.52±0.10*	0.65±0.36	5.48±0.18*	15.6±0.2	16.5±0.2
Leaf 5	29.5±0.7	18.5±0.3*	2.49±0.40**	1.96±0.22	0.62±0.25	5.72±0.04**	15.1±0.1*	18.1±0.2
Stem 1	33.1±1.9	24.8±1.4	3.28±0.53	2.38±0.49	1.38±0.10*	2.87±0.09**	16.5±2.7	18.5±1.2
Stem 2	31.9±2.4	22.0±1.6	2.80±0.25*	1.65±0.36	1.70±0.96	2.16±0.04**	19.3±0.2**	18.8±0.2*
Stem 3	28.9±1.5	19.3±1.1	2.30±0.40*	1.42±0.27	1.27±0.71	2.23±0.00**	20.0±0.6*	18.0±0.1
Stem 4	32.9±0.5**	21.0±0.4**	2.76±0.06	1.48±0.08	1.74±0.30	2.34±0.09**	19.4±0.4	13.3±0.1**
Stem 5	32.3±1.5*	20.1±0.9*	2.86±0.25	1.56±0.21	2.11±0.66	2.52±0.04	20.5±0.6*	14.6±0.1
Greenhouse								
Leaf 1	28.9±1.0	17.8±0.2	2.67±0.03	2.01±0.17	0.88±0.25	3.52±0.14	15.6±0.3	ND
Leaf 2	27.6±1.2	16.3±0.7	2.23±0.55	1.91±0.55	0.51±0.16	4.76±0.25	15.3±1.6	19.6[a]
Leaf 3	30.3±1.9	19.1±1.2	2.77±0.20	2.34±0.12	0.39±0.14	2.39±0.32	15.3±0.5	18.0[a]
Leaf 4	31.4±0.5	19.1±0.2	2.84±0.15	2.25±0.13	0.62±0.53	6.32±0.01	14.5±2.6	19.3[a]
Leaf 5	27.8±0.5	15.4±0.3	2.12±0.46	1.79±0.39	0.34±0.13	6.57±0.07	14.1±0.1	18.9[a]
Stem 1	31.8±3.1	23.4±2.1	2.86±0.28	2.19±0.27	0.45±0.16	4.76±0.25	15.4±0.5	18.6±0.3
Stem 2	31.4±3.8	22.3±3.0	2.53±0.31	1.75±0.24	0.96±0.38	4.72±0.05	16.0±0.1	16.5±0.1
Stem 3	26.6±1.0	17.8±0.6	1.78±0.27	1.15±0.42	0.50±0.12	3.58±0.02	17.5±0.6	17.2±0.5
Stem 4	39.1±0.8	24.9±0.5	2.90±0.14	1.56±0.12	0.46±0.25	3.14±0.02	17.4±1.2	17.8±0.7
Stem 5	40.3±1.2	23.7±0.4	2.72±0.08	1.36±0.11	1.05±0.29	2.59±0.20	18.4±0.3	16.0±0.8

Mean value±standard deviation

ND not determined

*$P \leq 0.05$; **$P \leq 0.01$ for field components when compared to greenhouse components

[a] No standard deviation because only a single replicate was available

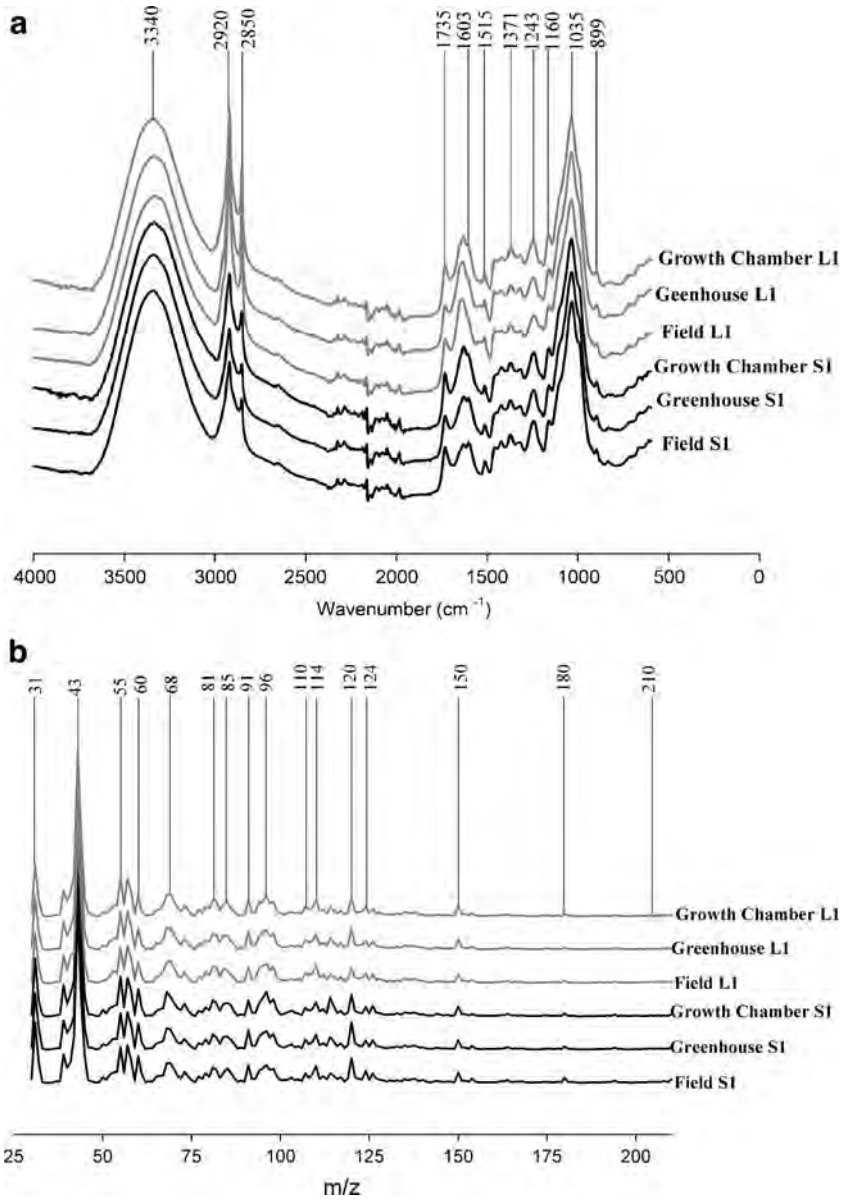

Fig. 3 **a** FTIR spectra collected on leaf 1 (*L1*) and Stem 1 (*S1*) of switchgrass grown under three different environmental conditions. **b** MBMS spectra collected on leaf 1 (*L1*) and stem 1 (*S1*) of switchgrass grown under three different environmental conditions

(cellulose, hemicelluloses, and lignin [30, 44]). The band at 3,340 cm^{-1} is assigned to hydroxyl groups, and the bands at 2,920 and 2,850 attributed to C–H groups. The band located at 1,735 cm^{-1} demonstrates the presence of carbonyl groups in hemicelluloses and lignin. The two absorbances at 1,603 and 1,515 cm^{-1} are the result of the breathing mode of the aromatic rings in lignin. Figure 3b shows the MBMS spectra resulting from switchgrass pyrolysis. The figures show that content features originated from undecomposed switchgrass components. Various masses can be specifically attributed to cellulose, hemicellulose, guaiacyl lignin, and syringyl lignin. Cellulose has mass peaks (*m*/*z*) values of 57, 60, 73, 85, 86, 96, 98, 100, 102, 110, 112, 126, and 144. Hemicellulose produces mass peaks values of 58, 85, 86, and 114. Whereas mass peaks of guaiacyl lignin have *m*/*z* values of 124, 137, 138, 150, 152, 164, 166, 178, and 180, syringyl lignin has *m*/*z* values of 154, 167, 168, 180, 182, 194, 208, and 210 [39, 48, 50].

From the MBMS spectra, the ratio between syringyl and guaiacyl units in core lignin (S/G ratio) was calculated and compared for different tiller components and different growth environments (Table 2). The differences between the average S/G ratio for leaves and the average S/G ratio for stems were significant ($P \leq 0.05$) for all three growth environments. Additionally, the total average S/G ratio (combined for leaves and stems) was significantly lower in growth chamber when compared to field and greenhouse ($P \leq 0.05$). From the FTIR spectra, absorbance ratios between peaks around 1,500 and 1,600 cm^{-1} were calculated to estimate the relative level

Table 2 The mean value of S/G ratios for individual components of plants grown in different environments

Component	Average S/G ratio		
	Field	Greenhouse	Growth Chamber
L1	0.44[a]	0.40[b]	0.35[b]
L2	0.39[a]	0.36[ab]	0.32[b]
L3	0.40[a]	0.37[ab]	0.35[b]
L4	0.36[a]	0.34[a]	0.33[a]
L5	0.34[a]	0.36[a]	0.34[a]
L6	0.36[a]	0.38[a]	0.34[a]
L7	0.45[a]	0.40[a]	0.40[a]
S1	0.47[a]	0.45[a]	0.36[b]
S2	0.49[a]	0.42[ab]	0.40[b]
S3	0.56[a]	0.52[ab]	0.42[b]
S4	0.57[a]	0.57[a]	0.46[b]
S5	0.56[a]	0.60[a]	0.52[a]
S6	0.59[a]	0.64[a]	0.51[b]
S7	0.62[a]	0.63[a]	0.52[b]
Total Average	0.48[a]	0.46[a]	0.40[b]

Letter groupings were obtained from mean separation test (Fisher's least significant difference method, $P \leq 0.05$) comparing single component (e.g., "L1") mean values across the three environments (field vs. greenhouse vs. growth chamber)

of cross-linked lignin present in the biomass (Table 3) as previously demonstrated [51]. A high 1,500/1,600 ratio has been linked to more condensed and cross-linked lignin structures [52]. In stem tissues, the ratio was found to significantly increase in field samples when compared to greenhouse and growth chamber samples, and in leaves, the ratio significantly increased in field and greenhouse samples when compared to growth chamber samples.

Spectroscopic approaches were undertaken to developed models that will be useful to predict lignin content in unknown samples. The models (FTIR and MBMS) were constructed by correlating each spectral data set to lignin content by partial least square regression technique. Figures 4a and 5a show the calibration and cross-validation models for FTIR and MBMS, respectively. The predicted values of lignin are plotted against the measured values to visualize the prediction performance. In such plots, the data should fall on the diagonal (target line) when a calibration model predicts the data perfectly. To evaluate the prediction performance of each calibration model, a cross-validation was performed on all samples. The procedure involves using a single observation from the original sample as the validation data and the remaining observations as the training data. This step is repeated such that each observation in a sample set is used once as the validation data. Various parameters can be calculated to determine a model's ability to fit the data and its predictive power, such as calibration R (coefficient of correlation for calibration) and cross-validation R (coefficient of correlation for cross-validation). In addition, the root mean square error of calibration (RMSEC) for the training data and the root mean square error of prediction (RMSEP) for the test data can be used to evaluate the quality of the models. For both models, an $R>0.94$ was obtained, and RMSEC and RMSEP were very low (<1%). A regression coefficient plot is an additional plot generated during a PLS model construction. This plot shows the chemical features that are responsible for the correlation between the spectral data of the samples and the predicted characteristics (lignin content). Figures 4b and 5b show the regression coefficients for the PLS models developed from the FTIR and MBMS data, respectively. Several absorbance bands in the mid-infrared region (1,735, 1,616, 1,507, 1,323 cm^{-1}) confirmed that lignin bands were used to build the models. The same observations can be made for the MBMS model. The masses at 137, 154, 167, 180, 194, 210, and others are found to contribute to the model. The FTIR and MBMS models were applied to predict lignin in switchgrass samples that were grown in the growth chamber. The content was predicted for the various components of the

Table 3 Measurement of lignin absorbances from the FTIR spectra of switchgrass plants grown in different environments

	Lignin absorbance at 1515cm^{-1}	Lignin absorbance at 1603cm^{-1}	Absorbance ratio between 1515 and 1603cm^{-1}
Stem			
Field	0.665±0.037	0.858±0.067	0.768±0.041[a]
Greenhouse	0.705±0.032	0.998±0.065	0.702±0.037[b]
Growth Chamber	0.715±0.029	1.004±0.094	0.713±0.061[b]
Leaf			
Field	0.748±0.090	1.058±0.086	0.719±0.042[b]
Greenhouse	0.847±0.062	1.266±0.046	0.685±0.065[b]
Growth Chamber	0.711±0.091	1.193±0.091	0.609±0.068[c]

Each data point is the mean±standard deviation of absorbances from at least five separate FTIR spectra. Letter groupings were obtained from mean separation test (Fisher's least significant difference method, $P \leq 0.05$)

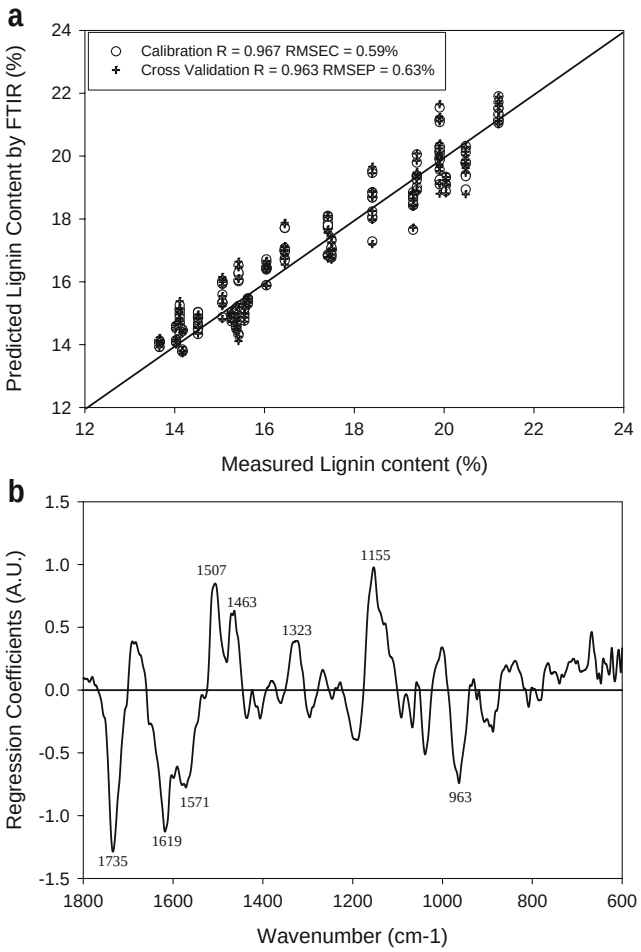

Fig. 4 **a** Results of a FTIR PLS model showing the correlation between the measured and predicted lignin content in switchgrass. **b** Regression coefficient plot from the FTIR PLS model allowing the identification of the most important variables in building the model

plant (leaf and stem tissues) and then compared to the value obtained by wet chemistry. Table 4 shows the results, the lignin content associated with a standard deviation predicted by FTIR, MBMS, and the "true" lignin content (wet chemistry).

From Table 4, several trends in lignin content were revealed from various tissues. For leaf tissues, no significant differences were seen for leaf tissue from the top of the tiller (L1) compared to all other leaf tissues down to the bottom of the tiller (L5). However, stem tissues had significantly increased in lignin content progressing from the top of the tiller (S1) to the bottom (S5). Similar results were observed for all environments (field, greenhouse, and growth chamber) from the wet chemistry results (Fig. 6a, b). The leaves displayed minimal differences between the different growth environments (Fig. 6b), while the stem regions showed significantly higher levels of lignin in the lower, more mature stem tissues (Fig. 6a). In addition, the younger stem tissues (S1, S2, and S3) from the field samples were characterized by slightly higher lignin levels when compared to the greenhouse and growth chamber samples.

Discussion

The percentage of biomass component (leaf versus stem) observed from the field in these experiments is comparable to other studies of switchgrass harvested in the spring and fall [18]. The percentage of biomass, composed of stems and leaves, is of relative importance to those involved in the processes within a biorefinery, resulting from the variation in chemical composition between different components (Fig. 2). For instance, 75% of the total biomass (excluding the panicle) from the field was composed of the stem tissue, containing an average of 19% lignin as measured by wet

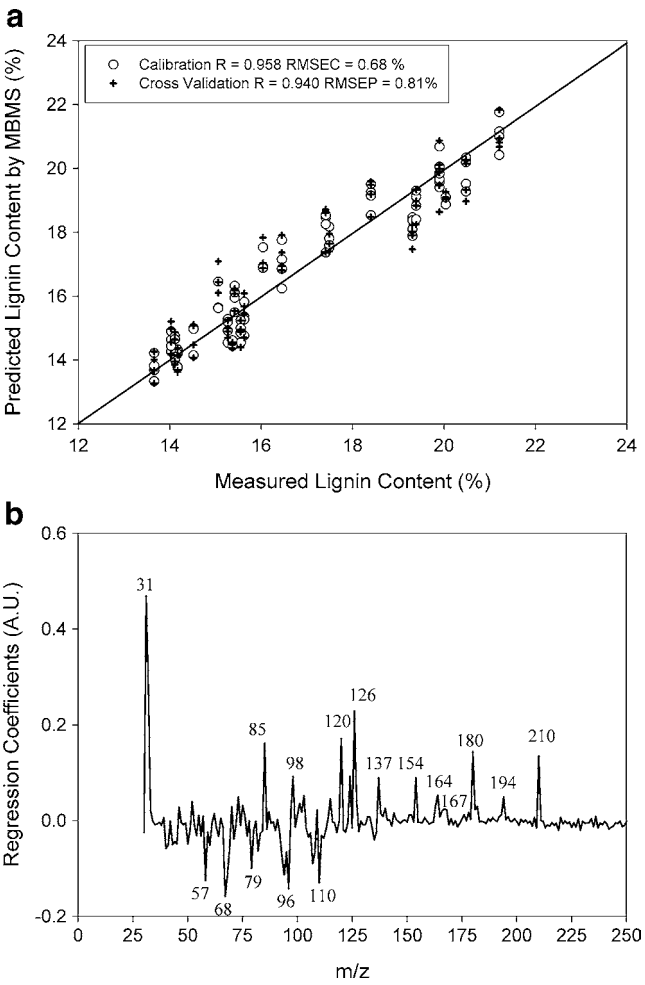

Fig. 5 **a** Results of a MBMS PLS model showing the correlation between the measured and predicted lignin content in switchgrass. **b** Regression coefficient plot from the MBMS PLS model allowing the identification of the most important variables in building the model

Table 4 Prediction of lignin content in switchgrass samples grown in growth chamber by FTIR and MBMS models with standard deviation in parenthesis

Growth chamber switchgrass	Predicted lignin content by FTIR (%)	Predicted lignin content by MBMS (%)	Calculated lignin content by wet chemistry (%)
L1	15.03 (1.09)	14.32 (0.80)	14.95 (0.39)
L2	13.65 (0.94)	15.42 (0.69)	14.87 (0.28)
L3	14.15 (1.15)	15.31 (0.67)	14.91 (0.26)
L4	14.07 (1.39)	14.75 (0.96)	14.55 (0.44)
L5	13.96 (1.39)	14.50 (0.75)	14.38 (0.11)
S1	14.15 (1.12)	15.54 (0.77)	14.40 (0.25)
S2	15.22 (0.77)	16.59 (0.77)	17.16 (0.21)
S3	16.60 (0.50)	17.09 (0.63)	17.75 (0.17)
S4	17.57 (0.48)	18.36 (0.53)	19.00 (0.04)
S5	17.79 (0.63)	18.77 (0.70)	19.07 (0.13)
S6	18.06 (0.82)	18.86 (0.86)	–
S7	18.30 (0.75)	19.44 (0.70)	–

chemistry (Table 1). However, the other 25% of the biomass, composed of leaves, only contains an average of 14.5% lignin. These differences are substantial and can have a significant impact on the performance of the biomass in a biorefinery.

Lignin levels are consistently higher in stem tissues when compared to leaf tissues [20, 21, 53], and these trends were noticeable in this study as well. The gradual increase in lignin moving from S1 down to S5 was observed in all three environments where switchgrass was grown and is consistent with results shown from a previous study [24]. There was a lack of variation in lignin content among different leaves throughout the switchgrass tiller (L1 to L5), although these results are not surprising, since switchgrass leaves do not play a major role in physically supporting the plant and do not undergo secondary growth.

Most striking are the significant differences observed between the overall S/G ratios (Table 2) and the cross-linking ratios (Table 3) when comparing the field and greenhouse to the growth chamber samples. Additionally, the percentage of stem biomass decreased from the field (75%) to the greenhouse (65%) to the growth chamber plants (56%). These patterns of differences between the switchgrass grown in the field, the greenhouse, and the growth chamber can most likely be attributed to inherent differences in the environments themselves. Plants within the environmentally controlled growth chambers are limited by the physical space available (e.g., the height of the switchgrass plants rapidly reaches the chamber ceiling, attaining a growth limitation within the chamber). This might explain the lower S/G ratios seen for samples from the growth chamber, as S/G ratios have been demonstrated to increase with stem development, and lower S/G ratios have been associated with less mature stem regions [5]. It is also likely that compositional differences observed between field-grown and growth chamber-grown switchgrass can be attributed to more environmental and mechanical stresses present in the field. Similar observations have been demonstrated to affect the chemical properties and lignin

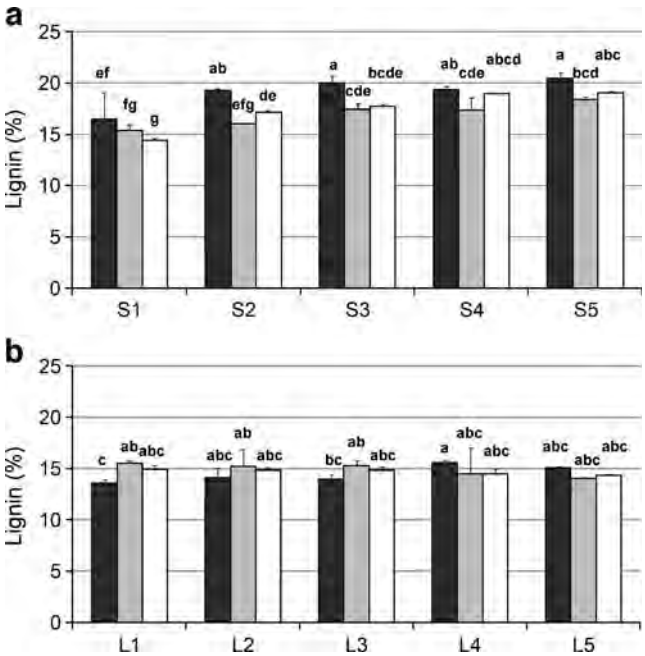

Fig. 6 **a** Lignin content (%) determined by wet chemistry of individual stem tissues (*S1* to *S5*) for switchgrass grown in the field (*black*), greenhouse (*gray*), and growth chamber (*white*). Letter groupings were obtained from mean separation test (Fisher's least significant difference method, $P \leq 0.05$). **b**. Lignin content (%) determined by wet chemistry of individual leaf tissues (*L1* to *L5*) for switchgrass grown in the field (*black*), greenhouse (*gray*), and growth chamber (*white*). Letter groupings were obtained from mean separation test (Fisher's least significant difference method, $P \leq 0.05$)

composition of pine and other trees [54, 55] and could have similar effects in herbaceous crops. These findings are necessary to take into account for studies where growth chambers will be used for initial assessments of traits (e.g., reduced lignin content) that are eventually desirable in field-grown energy crops. Observations made in the growth chamber may not be directly extrapolated to the field.

The FTIR and MBMS models were developed independently of the type of tissue and growth environment. The strong correlations obtained between the spectral data and the lignin content confirm that the techniques and the models are reliable to determine lignin content in plant tissues and to assess lignin chemical structures. The two high throughput techniques generate complimentary data that permit a more complete assessment of lignin in switchgrass. In addition to chemical composition, they provide information about physical and structural properties of biomass that directly influence biomass utilization and conversion. In conclusion, these techniques can be used to rapidly assess switchgrass biomass grown under different environments, determine the lignin complexity and content, and identify fluctuation among these parameters.

Acknowledgments The authors would like to acknowledge Mitra Mazarei and Murali Raghavendra for input on the manuscript. This work was funded by the Southeastern Sun Grant Initiative grant number DOT 0T0S5907G00050 and the Bioenergy Science Center (BESC). BESC is a US Department of Energy Bioenergy Research Center supported by the Office of Biological and Environmental Research in the DOE Office of Science.

References

1. Bransby DI, Ward CY, Rose PA, Sladden SE, Kee DD (1989) Biomass production from selected herbaceous species in the Southeastern USA. Biomass 20(1–2):187–197
2. McLaughlin SB, Ugarte DGDL, Garten CT, Lynd LR, Sanderson MA, Tolbert VR et al (2002) High-value renewable energy from prairie grasses. Environ Sci Technol 36(10):2122–2129
3. Schmer MR, Vogel KP, Mitchell RB, Perrin RK (2008) Net energy of cellulosic ethanol from switchgrass. PNAS 105(2):464–469
4. Lynd LR, Laser MS, Bransby D, Dale BE, Davison B, Hamilton R et al (2008) How biotech can transform biofuels. Nat Biotechnol 26(2):169–172
5. Chen L, Auh C, Chen F, Cheng X, Aljoe H, Dixon RA et al (2002) Lignin deposition and associated changes in anatomy, enzyme activity, gene expression, and ruminal degradability in stems of tall fescue at different developmental stages. J Agric Food Chem 50(20):5558–5565
6. Dixon RA, Chen F, Guo D, Parvathi K (2001) The biosynthesis of monolignols: a "metabolic grid", or independent pathways to guaiacyl and syringyl units? Phytochemistry 57(7):1069–1084
7. Vogel KP, Pedersen JF, Masterson SD, Toy JJ (1999) Evaluation of a filter bag system for NDF, ADF, and IVDMD forage analysis. Crop Sci 39(1):276–279
8. Yuan JS, Tiller KH, Al-Ahmad H, Stewart NR, Stewart CN Jr (2008) Plants to power: bioenergy to fuel the future. Trends Plant Sci 13(8):421–429
9. Sticklen MB (2008) Plant genetic engineering for biofuel production: towards affordable cellulosic ethanol. Nat Rev Genet 9(6):433–443
10. Alexandrova KS, Denchev PD, Conger BV (1996) Micropropagation of switchgrass by node culture. Crop Sci 36(6):1709–1711
11. Denchev PD, Conger BV (1994) Plant-regeneration from callus-cultures of switchgrass. Crop Sci 34(6):1623–1627
12. Richards HA, Rudas VA, Sun H, McDaniel JK, Tomaszewski Z, Conger BV (2001) Construction of a GFP-BAR plasmid and its use for switchgrass transformation. Plant Cell Rep 20(1):48–54
13. Somleva MN, Tomaszewski Z, Conger BV (2002) Agrobacterium-mediated genetic transformation of switchgrass. Crop Sci 42(6):2080–2087
14. Tobias CM, Twigg P, Hayden DM, Vogel KP, Mitchell RM, Lazo GR et al (2005) Analysis of expressed sequence tags and the identification of associated short tandem repeats in switchgrass. Theor Appl Genet 111(5):956–964
15. Alexandrova KS, Denchev PD, Conger BV (1996) In vitro development of inflorescences from switchgrass nodal segments. Crop Sci 36(1):175–178
16. Denchev PD, Conger BV (1995) In-vitro culture of switchgrass—influence of 2, 4-D and picloram in combination with benzyladenine on callus initiation and regeneration. Plant Cell Tiss Org 40(1):43–48
17. Sladden SE, Bransby DI, Aiken GE (1991) Biomass yield, composition and production costs for 8 switchgrass varieties in Alabama. Biomass Bioenerg 1(2):119–122
18. Adler PR, Sanderson MA, Boateng AA, Weimer PI, Jung HJG (2006) Biomass yield and biofuel quality of switchgrass harvested in fall or spring. Agron J 98(6):1518–1525
19. Dien BS, Jung HJG, Vogel KP, Casler MD, Lamb JFS, Iten L et al (2006) Chemical composition and response to dilute-acid pretreatment and enzymatic saccharification of alfalfa, reed canarygrass, and switchgrass. Biomass Bioenerg 30(10):880–891
20. Grabber JH, Jung GA, Hill RR (1991) Chemical-composition of parenchyma and sclerenchyma cell-walls isolated from orchardgrass and switchgrass. Crop Sci 31(4):1058–1065
21. Law KN, Kokta BV, Mao CB (2001) Fibre morphology and soda-sulphite pulping of switchgrass. Bioresource Technol 77(1):1–7
22. El-Nashaar HM, Banowetz GM, Griffith SM, Casler MD, Vogel KP (2009) Genotypic variability in mineral composition of switchgrass. Bioresource Technol 100(5):1809–1814
23. Sarath G, Mitchell RB, Sattler SE, Funnell D, Pedersen JF, Graybosch RA et al (2008) Opportunities and roadblocks in utilizing forages and small grains for liquid fuels. J Ind Microbiol Biotechnol 35(5):343–354
24. Sarath G, Baird LM, Vogel KP, Mitchell RB (2007) Internode structure and cell wall composition in maturing tillers of switchgrass (*Panicum virgatum.* L). Bioresource Technol 98 (16):2985–2992
25. Meuzelaar HLC, Haverkamp J, Hileman FD (1982) Pyrolysis mass spectrometry of recent and fossil biomaterials. Elsevier, New York
26. Goodacre R, Timmins EM, Burton R, Kaderbhai N, Woodward AM, Kell DB et al (1998) Rapid identification of urinary tract infection bacteria using hyperspectral whole-organism fingerprinting and artificial neural networks. Microbiol-UK 144:1157–1170
27. Smedsgaard J, Frisvad JC (1996) Using direct electrospray mass spectrometry in taxonomy and secondary metabolite profiling of crude fungal extracts. J Microbiol Meth 25(1):5–17
28. van Baar BLM (2000) Characterization of bacteria by matrix-assisted laser desorption/ionisation and electrospray mass spectrometry. FEMS Microbiol Rev 24(2):193–219
29. del Rio JC, Gutiérrez A, Romero J, Martínez MJ, Martínez AT (2001) Identification of residual lignin markers in eucalypt kraft pulps by Py-GC/MS. J Anal Appl Pyrol 58–59:425–439
30. Faix O, Bremer J, Schmidt O, Stevanovic T (1991) Monitoring of chemical changes in white-rot degraded beech wood by

pyrolysis–gas chromatography and Fourier-transform infrared spectroscopy. J Anal Appl Pyrol 21:147–162
31. Faix O, Meier D, Grobe I (1987) Studies on isolated lignins and lignins in woody materials by pyrolysis–gas chromatography–mass spectrometry and off-line pyrolysis–gas chromatography with flame ionization detection. J Anal Appl Pyrol 11:403–416
32. Izumi A, Kuroda K, Ohi H, Yamaguchi A (1995) Structural analysis of lignin by pyrolysis–gas chromatography. III. Comparative studies of pyrolysis–gas chromatography and nitrobenzene oxidation for the determination method of lignin comosition in hardwood. Jpn Tappi 49(9):1339–1346
33. Martin F, Saiz-Jimenez C, Gonzalez-Vila FJ (1979) Pyrolysis–gas chromatography–mass spectrometry of lignins. Holzforschung 33 (6):210–212
34. Rodrigues J, Graca J, Pereira H (2001) Influence of tree eccentric growth on syringyl/guaiacyl ratio in *Eucalyptus globulus* wood lignin assessed by analytical pyrolysis. J Anal Appl Pyrol 58–59:481–489
35. Rodrigues J, Meier D, Faix O, Pereira H (1999) Determination of tree-to-tree variation in syringyl/guaiacyl ratio of *Eucalyptus globulus* wood lignin by analytical pyrolysis. J Anal Appl Pyrol 48(2):121–128
36. Sonoda T, Ona T, Yokoi H, Ishida Y, Ohtani H, Tsuge S (2001) Quantitative analysis of detailed lignin monomer composition by pyrolysis-gas chromatography combined with preliminary acetylation of the samples. Anal Chem 73(22):5429–5435
37. Agblevor FA, Evans RJ, Johnson KD (1994) Molecular-beam mass-spectrometric analysis of lignocellulosic materials. 1. Herbaceous biomass. J Anal Appl Pyrol 30(2):125–144
38. Davis MF, Megraw R, Sewell M, Evans R, Neale D, West D, et al (1999) Application of pyrolysis molecular beam mass spectrometry for the determination of loblolly pine and hybrid poplar cell wall composition. Paper presented at the TAPPI Pulping Conference, Orlando, FL, 31 October–4 November 1999 3: 1077–1081
39. Evans RJ, Milne TA (1987) Molecular characterization of the pyrolysis of biomass. 2. Applications. Energ Fuel 1(4):311–319
40. Evans RJ, Milne TA, Soltys MN (1986) Direct mass-spectrometric studies of the pyrolysis of carbonaceous fuels. III. Primary pyrolysis of lignin. J Anal Appl Pyrol 9(3):207–236
41. Kelley SS, Jellison J, Goodell B (2002) Use of NIR and pyrolysis-MBMS coupled with multivariate analysis for detecting the chemical changes associated with brown-rot biodegradation of spruce wood. FEMS Microbiol Lett 209(1):107–111
42. Davis MF, Tuskan GA, Payne P, Tschaplinski TJ, Meilan R (2006) Assessment of Populus wood chemistry following the introduction of a Bt toxin gene. Tree Physiol 26(5):557–564
43. Sykes R, Kodrzycki B, Tuskan GA, Foutz K, Davis M (2008) Within tree variability of lignin composition in *Populus*. Wood Sci Technol 42(8):649–661
44. Labbé N, Rials TG, Kelley SS, Cheng ZM, Kim JY, Li Y (2005) FT-IR imaging and pyrolysis–molecular beam mass spectrometry: new tools to investigate wood tissues. Wood Sci Technol 39 (1):61–76
45. Chen L, Carpita NC, Reiter WD, Wilson RH, Jeffries C, McCann MC (1998) A rapid method to screen for cell-wall mutants using discriminant analysis of Fourier transform infrared spectra. Plant J 16(3):385–92
46. Kataoka Y, Kondo T (1999) Quantitative analysis for the cellulose I alpha crystalline phase in developing wood cell walls. Int J Biol Macromol 24(1):37–41
47. Moore KJ, Moser LE, Vogel KP, Waller SS, Johnson BE, Pedersen JF (1991) Describing and quantifying growth stages of perennial forage grasses. Agron J 83(6):1073–1077
48. Evans RJ, Milne TA (1987) Molecular characterization of the pyrolysis of biomass. Energ Fuel 1(2):123–137
49. Tuskan G, West D, Bradshaw HD, Neale D, Sewell M, Wheeler N et al (1999) Two high-throughput techniques for determining wood properties as part of a molecular genetics analysis of hybrid poplar and loblolly pine. Appl Biochem Biotechnol 77(1–3):55–65
50. Shin EJ, Hajaligol MR, Rasouli F (2003) Characterizing biomatrix materials using pyrolysis molecular beam mass spectrometer and pattern. J Anal Appl Pyrol 68–69:213–229
51. Stewart D, Yahiaoui N, McDougall GJ, Myton K, Marque C, Boudet AM et al (1997) Fourier-transform infrared and Raman spectroscopic evidence for the incorporation of cinnamaldehydes into the lignin of transgenic tobacco (*Nicotiana tabacum* L.) plants with reduced expression of cinnamyl alcohol dehydrogenase. Planta 201(3):311–318
52. Zhong R, Morrison WH III, Himmelsbach DS, Poole FL II, Ye Z-H (2000) Essential role of caffeoyl coenzyme A *O*-methyltransferase in lignin biosynthesis in woody poplar plants. Plant Physiol 124 (2):563–577
53. Jung HJG, Vogel KP (1992) Lignification of switchgrass (*Panicum virgatum*) and big bluestem (*Andropogon gerardii*) plant-parts during maturation and its effect on fiber degradability. J Sci Food Agr 59(2):169–176
54. Okuyama T, Takeda H, Yamamoto H (1998) Relation between growth stress and lignin concentration in the cell wall: ultraviolet microscopic spectral analysis. J Wood Sci 44(2):83–89
55. Yeh T-F, Goldfarb B, Chang H-M, Peszlen I, Braun JL, Kadla JF (2005) Comparison of morphological and chemical properties between juvenile wood and compression wood of loblolly pine. Holzforschung 59(6):669–674